Convergent trends and spatiotemporal patterns of arboviruses in Mexico and Central America

Bernardo Gutierrez[1,2,*], Darlan da Silva Candido[1,3], Sumali Bajaj[1], Abril Paulina Rodriguez Maldonado[4], Fabiola Garces Ayala[4], María de la Luz Torre Rodriguez[4], Adnan Araiza Rodriguez[4], Claudia Wong Arámbula[4], Ernesto Ramírez González[4], Irma López Martínez[4], José Alberto Díaz-Quiñónez[4,5], Mauricio Vázquez Pichardo[4], Sarah C. Hill[6], Julien Thézé[7], Nuno R. Faria[1,3,8,9], Oliver G. Pybus[1,6], Lorena Preciado-Llanes[10], Arturo Reyes-Sandoval[10,11], Moritz U.G. Kraemer[1,*], Marina Escalera-Zamudio[1,*]

[1]*Department of Biology, University of Oxford, UK*
[2]*Colegio de Ciencias Biológicas y Ambientales, Universidad San Francisco de Quito USFQ, Ecuador*
[3]*Instituto de Medicina Tropical, Faculdade de Medicina da Universidade de São Paulo, Brazil*
[4]*Instituto de Diagnóstico y Referencia Epidemiológicos (InDRE) "Dr. Manuel Martínez Báez", Secretaría de Salud, México.*
[5]*Instituto de Ciencias de la Salud, Universidad Autónoma del Estado de Hidalgo, Mexico*
[6]*Department of Pathobiology and Population Sciences, Royal Veterinary College, London, UK*
[7]*Université Clermont Auvergne, INRAE, VetAgro Sup, UMR EPIA, Saint-Genès-Champanelle, France*
[8]*MRC Centre for Global Infectious Disease Analysis, School of Public Health, Imperial College London, London, UK*
[9]*The Abdul Latif Jameel Institute for Disease and Emergency Analytics, School of Public Health, Imperial College London, London, UK*
[10]*Nuffield Department of Medicine/Wellcome Centre for Human Genetics, University of Oxford, UK*
[11]*Instituto Politécnico Nacional (IPN), Av. Luis Enrique Erro s/n., Unidad Adolfo López Mateos, Mexico City, Mexico*

**Corresponding authors: bernardo.gutierrez@biology.ox.ac.uk, moritz.kraemer@biology.ox.ac.uk, marina.escalerazamudio@biology.ox.ac.uk*

ABSTRACT (269 words)

Background:
Arboviruses cause both seasonal epidemics (e.g. dengue viruses, DENV) and emerging outbreaks (e.g. chikungunya and Zika viruses, CHIKV and ZIKV) with a significant impact on global health. These viruses share mosquito vector species, often infecting the same host population within overlapping geographic regions. Thus, comparative analyses of their evolutionary and epidemiological dynamics across spatial and temporal scales could reveal convergent transmission trends.

Methodology/Principal Findings:
Focusing on Mexico as a case study, we generated CHIKV, DENV-1 and DENV-2 genomes from an epidemiological surveillance-derived historical sample collection, and analysed them together with longitudinally-collected genome and epidemiological data from the Americas. Arboviruses endemically circulating within the country were found to be introduced multiple times from lineages predominantly sampled from the Caribbean and Central America. For CHIKV, at least thirteen introductions were inferred over a year, with six of these leading to persistent transmission chains. For both DENV-1 and DENV-2, at least seven introductions were inferred over a decade.

Conclusions/Significance:
Our results suggest that CHIKV, DENV-1 and DENV-2 in Mexico share similar evolutionary and epidemiological trajectories. The southwest region of the country was determined to be the most likely location for viral introductions from abroad, with a subsequent spread into the Pacific coast towards the north of Mexico. The virus diffusion patterns observed across the country are likely driven by multiple factors, including mobility linked to human migration from Central towards North America. Considering Mexico's economic role and geographic positioning displaying a high human mobility across borders, our results prompt the need to better understand the role of anthropogenic factors in the transmission dynamics of arboviruses, particularly linked to land-based human migration.

AUTHOR SUMMARY (112 words)

Mexico is endemic to several mosquito-borne viruses relevant to global health, and ranks within the top five countries in the Americas that report the highest case numbers. Our study provides a general overview of arbovirus introduction, spread and establishment patterns in North and Central America, and should be of interest to both local health and global authorities. Moreover, it sets to explore the paradigm of convergence at different scales in independent virus populations, represented by comparable epidemiological and evolutionary trends in arboviruses sharing ecological niches. Our results represent important advances in the study of mosquito-borne viruses listed as a threat to global health, specifically applied to key countries within the developing world

MAIN TEXT: 5642 words

INTRODUCTION

Arbovirus spread is driven by a complex interaction between environmental conditions[1,2], ecological factors affecting vector populations [3,4], human behaviour and mobility [5–10], as well as pre-existing levels of immunity within the host population[11–13]. Whilst some arboviruses display seasonal dynamics with varying transmission peaks across time[14–17], novel and/or re-emerging viruses can cause explosive outbreaks in areas where the local population has limited or non-existent prior immunity[18–22]. Thus, untangling the individual contributions of the diverse drivers impacting viral spread across spatiotemporal scales remains a challenge. However, comparative phylodynamic approaches can provide a powerful tool to identify shared epidemiological and evolutionary trends, offering valuable information to better understand current and future outbreaks. Moreover, mapping arboviral emergence and spread within specific regions can inform on the development of efficient, spatially targeted interventions, including widening genomic-epidemiology surveillance efforts, local campaigns for vector control/clearance, and targeted vaccination campaigns stratified by age group and location.

Apart from sharing vector species, arboviruses tend to circulate within the same host population and geographic region, and thus are expected to exhibit similar evolutionary and epidemiological trends (despite their specific disease dynamics likely to be shaped by previous and cross-immunity within the host population[23–25]). Highlighted by the recent introduction of the Zika (ZIKV) and chikungunya (CHIKV) mosquito-borne viruses into the Americas, exploring the evolutionary and epidemiological dynamics of established arboviruses that have circulated endemically over multiple decades within the region (such as dengue virus, DENV), could help identify recurrent patterns for emerging arboviruses.

In the Americas (ruling out possible unidentified chikungunya fever cases during the 17th and 19th centuries, originally likely misdiagnosed as dengue fever[26,27]), locally acquired CHIKV infections were first confirmed during the mid 2010s[28], after which large outbreaks were detected between 2013 to 2017. On the other hand, all DENV serotypes (DENV-1 to DENV-4) display a somewhat different epidemic history within the region. Dengue-like illness has been well documented since the late 1700s[29], yet a considerable epidemiological shift occurred after the establishment of larger and more frequent outbreaks recorded during the 1950-60s[30]. By the 1980-90s, DENV outbreaks were reported on a yearly basis in at least 24 countries, with virus re-emergence mostly driven by the re-establishment of the previously eradicated *Ae. aegypti* mosquito population following the ban of use of DDT in the 1970s [30] (for a detailed description see Supplementary Text 1).

In Mexico, arbovirus surveillance takes place under the National Epidemiological Surveillance System ('Sistema Nacional de Vigilancia Epidemiológica – SINAVE') [31]. Following this scheme, CHIKV surveillance formally commenced in late 2014, with a high number of cases detected during 2015, particularly in the southern and southwestern states of the country [32]. On the other hand, the longitudinal surveillance of DENV shows that serotypes 1, 2 and 4 co-circulated in the country since the 1980s[33], whilst DENV-3 was first detected in 1995 [34]. Given ideal ecological and climatic conditions favouring vector populations, the south coast region of the country (comprising the states of Chiapas, Oaxaca, Guerrero, Veracruz, Tamaulipas, Quintana Roo, Campeche and Yucatán) has been historically the most affected by arboviruses [33,34]. Of interest, the spread of CHIKV and ZIKV across the country coincided with a decrease in DENV incidence observed for these states, with a low in cases recorded during the peak of both the CHIKV and ZIKV epidemics[35].

Historical samples linked to cases officially reported under the SINAVE represents a valuable tool for retrospectively exploring epidemiological and evolutionary dynamics of arboviruses circulating in Mexico. In this light, we present a new set of 39 CHIKV, 7 DENV-1 and 11 DENV-2 partial and complete viral genomes derived from samples catalogued under the SINAVE, collected between 2013 and 2017 across different states of the country. Under the hypothesis that the evolutionary and epidemiological dynamics of different arboviruses circulating in the Americas may display converging trends, we used a phylogeographic approach to analyse diversely sourced genome data from the region (including the genomes generated here), with a particular focus on quantifying lineage importations into Mexico. By interpreting our results alongside longitudinal epidemiological data, we compare the spatial epidemiology of these three viruses, and further assess extrinsic factors that are likely driving their dynamics. We find important similarities between the introduction of DENV and CHIKV into the country across different spatial and temporal scales.

METHODS

Sample selection and virus genome sequencing

Under SINAVE[31], the National Arbovirus Reference Laboratory (World Health Organization Collaborating Centre at the 'Instituto de Diagnóstico y Referencia Epidemiológicos Dr. Manuel Martínez Báez – InDRE', Ministry of Health of Mexico, Mexico City) stores a proportion of samples from confirmed DENV, CHIKV and ZIKV cases recorded nationally, collected by the national network of public health laboratories (RNLSP). For this purpose, positive serum samples are periodically shipped from state laboratories across the country to InDRE, where they are processed using reference molecular methods for epidemiological surveillance, and stored long-term (over a temporal span of decades). This has resulted historic

collection of samples covering multiple years and locations, and includes associated epidemiological and demographic data.

Derived from this collection, we sequenced a set of both human and mosquito-derived DENV and CHIKV virus genomes from samples selected based on their geographic location and collection date (Table S1). Initially, ZIKV samples were also considered, but failed to amplify under the multiplexed PCR described below. Briefly, candidate samples were first selected by identifying those with sampling dates and locations poorly represented by publicly available genomic data from Mexico (https://www.ncbi.nlm.nih.gov/genbank/). Samples were further selected based on the initial diagnostic qPCR C_t values ($C_t \leq 35$). Total RNA was used to generate cDNA using the SuperScript™ IV First-Strand Synthesis System (Invitrogen, CA, USA) with random hexamers, and subjected to multiplexed PCR reactions using virus-specific primer sets[43,44]. PCR products consisted of multiple overlapping ~400 nt fragments that cover the vast majority of the viral coding regions (excluding extreme ends). PCR reactions were performed using the Q5 High-Fidelity DNA polymerase kit (New England Biolabs, MA, USA) for 35-40 cycles, whilst products were purified using AmpureXP magnetic bead system (Beckman Coulter, CA, USA) to be quantified on the Qubit 3.0 using the Qubit dsDNA High Sensitivity kit (Life Technologies, CA, USA).

For viral genome sequencing, we used a ligation sequencing approach [45] on the MinION sequencing device (Oxford Nanopore Technologies, UK). Sequencing libraries were prepared from the purified PCR products using barcoding for individual samples (EXP-NBD104, EXP-NBD114, and SQK-LSK109 kits, Oxford Nanopore Technologies, UK). For sequencing, samples were pooled equimolarly to be loaded onto R9.4 flow cells (Oxford Nanopore Technologies, UK), with runs were carried out until a sequencing depth of >20X was achieved, monitored in real-time using the RAMPART platform (https://artic.network/ncov-2019/ncov2019-using-rampart.html).

Individual consensus viral genomes were assembled against designated reference sequences for each serotype under a >95% sequence identity threshold, whilst their assignment to specific viral genotypes was performed using the Arbovirus Typing Tools from the Genome Detective web server [46]. Virus genomes generated I this study are available as alignment provided in as **Supplementary Data 1-3.**

Phylogenetic analyses

Complete viral genome sequences from the Americas belonging to DENV-1 (Genotype V), DENV-2 (Genotype III) and CHIKV (Asian Genotype) available in GenBank (https://www.ncbi.nlm.nih.gov/genbank/) were retrieved to generate our datasets. High-quality sequences were included if collected from any country in North, Central and South America or the Caribbean as of 2020-02-01, and if >10,000 nt long. The DENV dataset was further expanded to include more sequences from Latin America, by adding 16 DENV-1 and 14 DENV-2 complete genomes from Nicaragua collected in between 2013 and 2019 (derived from a paediatric cohort that only became publicly available after initial sequence collation)[47,48]. In total, 420 CHIKV, 375 DENV-1 and 643 DENV-2 genome sequences were included in our final datasets (**Supplementary Data 4**). Each dataset was then aligned using *MAFFT*[49] and visually inspected, to be further trimmed to remove the untranslated terminal regions UTRs. Final alignments comprise a total length of 11,151 bp for CHIKV, 10,180 bp for DENV-1 and 10,023 bp for DENV-2. Maximum likelihood (ML) phylogenetic trees were then constructed using *IQtree 2.0*[50], resulting in a phylogeny for each virus. For each dataset, Maximum Likelihood trees were inferred under a General Time Reversible (GTR) substitution model, and the substitution rate heterogeneity across sites modelled under a Gamma distribution. Branch support was estimated using non-parametric Shimoda-Hasegawa approximate Likelihood Ratio Tests (SH-aLRTs) and

1000 replicates[51]. In order to identify general phylogenetic patters (including main virus clades), the resulting trees were midpoint rooted and annotated with the sequence collection date and location (country/region). To assess the temporal signal within the trees, plotted regressions between the tree tips to the tree root and their associated collection date were estimated using *TempEst v1.5.3*[52].

Time-calibrated phylogeographic analyses

To further explore the spatial and temporal dynamics of the viruses studied here, time-calibrated phylogenetic phylogenies were further estimated from the alignments described above with *BEAST v1.10.4*[53], using sequence collection dates to inform tree tip dates. For two DENV-1 genomes with no collection date available, a uniform prior was assigned to the corresponding tips. All trees were inferred using the Hasegawa-Kishino-Yano (HKY) substitution model with rate heterogeneity modelled under a Gamma distribution. Further, a Skyride tree prior[54] and a relaxed uncorrelated clock model[55] under a continuous-time Markov chain (CTMC) rate prior were implemented[56]. In each case, the Markov Chain Monte Carlo (MCMC) chains were run in duplicate for $1x10^8$ states, with the first $1x10^7$ discarded as a burn-in. Independent runs were combined using *LogCombiner*, resulting in an empirical distribution of 35,000 trees that was summarised into a Maximum Clade Credibility (MCC) tree with *TreeAnnotator*. Convergence was assessed for individual MCMC chains using *Tracer* [57], verifying that all relevant parameters achieved effective sample size (ESS) value of >200. For the DENV dataset, Tracer was also used to generate a Bayesian Skyline plot (BSP) for the MCC tree, used for evaluating changes in viral effective population size (Ne) across time under a coalescent model [58].

Virus diffusion patterns within Mexico and across bordering countries was explored using a discrete phylogeographic discrete trait analysis (DTA)[59]. Locations

assigned to tips correspond either to the country of collection, or to the geographic region within the country where the sequences were collected from (for Mexico sequences only) (**Table 1**). For this, the posterior tree sample was then resampled under an asymmetric substitution model for location reconstruction at ancestral nodes [59]. The statistical significance of transition rates between locations that best explain viral diffusion processes was evaluated under a Bayes Factor (BF) tests, explored through a Bayesian Stochastic Search Variable Selection (BSSVS) implemented in *BEAST* [59]. A criterion of a BF > 4 was used to define well-supported diffusion rates, together with a corresponding posterior probability (PP) of >0.5 [60]. The expected number of transitions between countries and regions was estimated for each virus subtype using a robust counting approach[61]. As in the previous step, MCC trees were generated by summarizing the posterior tree sample, further estimating posterior probabilities for inferred locations at given nodes.

Collation and analysis of historical epidemiological data

The SINAVE system collects arbovirus data at an individual case level using a digital platform in real time, made available to us through the National Institute for Epidemiological Diagnosis and Reference (InDRE) [31]. The database includes over 200 variables for officially confirmed DENV and CHIKV cases recorded between 2010 and 2019, such as clinical (date of symptom onset, date of sample collection, final diagnosis), demographic (patient age and sex) and geographic information (collection state, municipality and locality). Further, it also included serotype information for a proportion (approximately 10%) of positive DENV cases that are confirmed by serology or by PCR and product sequencing. Different variables were used to explore the epidemiological trends across time of the viruses studied here.

RESULTS

CHIKV genome data

From selected CHIKV samples collected from between May 2014 to December 2015 and 18/32 (56%) federal states in Mexico, we were able to generate 39 complete CHIKV genomes that were assigned to the Asian genotype, corresponding to the main genotype reported to circulate in the Americas [62] (**Supplementary Information, Table S1**). The set of newly generated viral genomes represent a substantial addition to previous publicly available data from Mexico, enhancing the geographical and spatio-temporal sampling range for CHIKV (**Table 1**). In this context, throughout the CHIKV outbreak in the Americas, genome availability across countries gradually increased through 2014, but was maintained at <10 sequences per month (**Supplementary Information, Fig S1**). Virus genomes from the USA, various Caribbean territories and Central American nations were made publicly available in that year, yet a limited number of genome sequences were generated from Mexico between 2014 and 2015. Overall, the number of genomes per country does not correlate with the cumulative number of cases reported over time (**Supplementary Information, Fig S2**).

Table 1. Arbovirus epidemiology across geographic regions in Mexico

Region	State	*CHIKV*		*DENV-1*		*DENV-2*	
		Cases[a]*	*Seqs*[c]	*Expected cases*[b]**	*Seqs*[c]	*Expected cases*[b]**	*Seqs*[c]
Northwest	Baja California Norte	905	2	16703	--	9522	--
	Baja California Sur						
	Chihuahua						
	Durango						
	Sinaloa						
	Sonora						
Northeast	Coahuila	240	4	6618	--	14207	--
	Nuevo León						
	Tamaulipas						
Centre-north	Aguascalientes	31	3	6749	--	314	--
	Guanajuato						
	Querétaro						
	San Luis Potosí						
	Zacatecas						
Centre-south	Mexico state	795	6	5613	1	1150	1
	Mexico City						
	Morelos						
West	Colima	2959	7	20145	3	8839	4
	Jalisco						
	Michoacán						
	Nayarit						
East	Hidalgo	2501	6	17267	1	10225	4
	Puebla						
	Tlaxcala						
	Veracruz						
Southwest	Chiapas	3951	12	9994	1	16150	6
	Guerrero						
	Oaxaca						
Southeast	Campeche	2276	7	12839	70	6384	11
	Quintana Roo						
	Tabasco						
	Yucatán						

*Source: SINAVE data, InDRE/Ministry of Health, Mexico.
**Calculated as the relative proportion of the serotype relative to all serotyped cases multiplied by the total of reported DF/DHF cases, rounded up. Source: SINAVE data, InDRE/Ministry of Health, Mexico.
[a]Reported between 2015 and 2018.
[b]Reported between 2013 to 2018.
[c]Including genomes generated in this study, plus previous publicly available genome data from Mexico.

Epidemiological dynamics of CHIKV in Central America and Mexico

The CHIKV epidemic in the Americas was well documented since its earliest detection in 2013 [39,63–69]. The first CHIKV cases were reported in the Eastern Caribbean (also named the Lesser Antilles (**Supplementary Information**, **Table S2**), likely leading to large outbreaks observed in other Central Caribbean islands (**Fig 1A**). During this early phase, the Dominican Republic (Central Caribbean) and Guadeloupe (Eastern Caribbean) reported over 15,000 new daily cases at their respective epidemic peaks occurring around July and December 2014 (Fig S1A). Following this, Central America and the Andean region of South America also experienced large outbreaks in 2015

and early 2016, but these were generally associated with lower case numbers (**Fig 1A**). Between March and December 2015, Colombia reported the largest number of cases within the region (**Supplementary Information**, **Fig S1A**). Subsequently, the southern cone region of South America (represented predominantly by Brazil) drove a resurgence of CHIKV cases in the continent over the following year (between March 2016 and January 2017) (**Fig 1A** and **Supplementary Information**, **Fig S1A**) [44,63,65,70–73].

The CHIKV epidemic in Mexico began approximately one year after the first the outbreaks recorded in the Caribbean islands during late 2013 [74,75]. Mexico reported CHIKV cases from the end of 2014 throughout 2018, with new cases rapidly increasing after January 2015 to reach a highest in the summer of the same year (**Fig 1B**). New case numbers grew from 506 (recorded in May) to around 2700 (recorded in August 2015). CHIKV cases increased in the Southwest region of the country, followed by infection peaks observed in the East (Gulf of Mexico) and West (Pacific Ocean) coast regions, as well as in the Southeast (encompassing the Yucatán peninsula) (**Fig 1C**). Limited numbers of cases were also observed in the centre-south region (comprising Mexico City and surrounding areas). Later, a small peak in cases was observed in the Northwest, representing the only region that saw a modest second wave of CHIKV cases during January 2017 (**Supplementary Information, Fig S3**).

Fig 1. CHIKV epidemiological trends in the Americas and Mexico from 2013 to 2018.

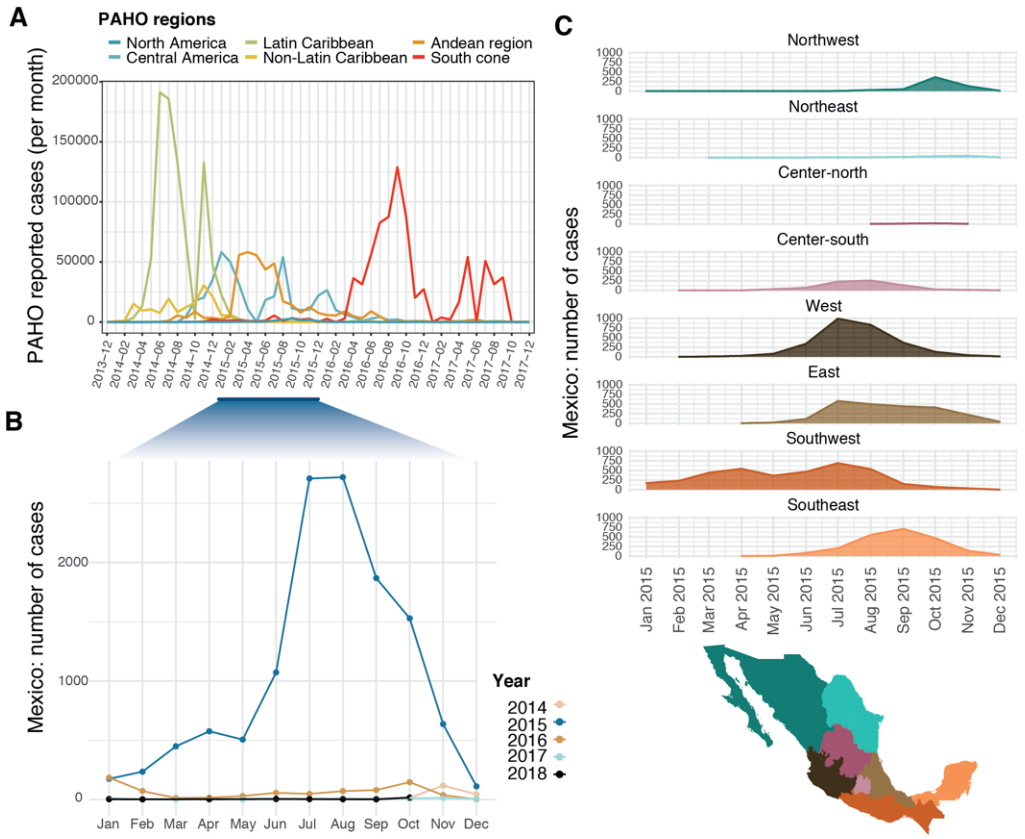

(A) Monthly number of CHIKV cases reported to the Pan-American Health Organisation (PAHO) between 2013 and 2017, grouped by PAHO region. The largest epidemic peak in Mexico (PAHO North America region) occurred in 2015, highlighted in blue. ***(B)*** Monthly number of confirmed CHIKV cases in Mexico grouped by year, as reported by the SINAVE. ***(C)*** Monthly number of confirmed CHIKV cases per geographic region in Mexico during 2015. A map of the states included in each geographic region is shown below. Details of the states included in each region are available in Table 1.

Evolutionary dynamics of CHIKV in Central America and Mexico

Our phylogenetic analysis shows that the CHIKV outbreak in the Americas was caused by a single virus lineage (SH-aLRT = 97.9, referred to here as the 'American' lineage). This lineage descends from sequences sampled from Southeast Asia and the Pacific Islands (**Fig 2A**), denoting a single introduction event of the CHIKV Asian genotype into the Americas. An early rapid expansion of CHIKV across North and South America is apparent at the base of the lineage, with an observed poorly supported clustering of sequences collected from different countries (**Supplementary Information, Fig S4**). Within the 'American' lineage, a large clade containing genome sequences

predominantly sampled from the Caribbean, Central America and North America was identified, including all sequences from Mexico (referred here to as the CCNA clade. SH-aLRT = 77.5) (Fig S4). Within the CCNA, the CHIKV genomes from Mexico mostly group into 6 well-supported clusters, grouping together other sequences from Central America and the Caribbean (**Fig 2** and **Supplementary Information, Fig S4**).

Fig 2. Time-scaled analysis for CHIKV in Mexico

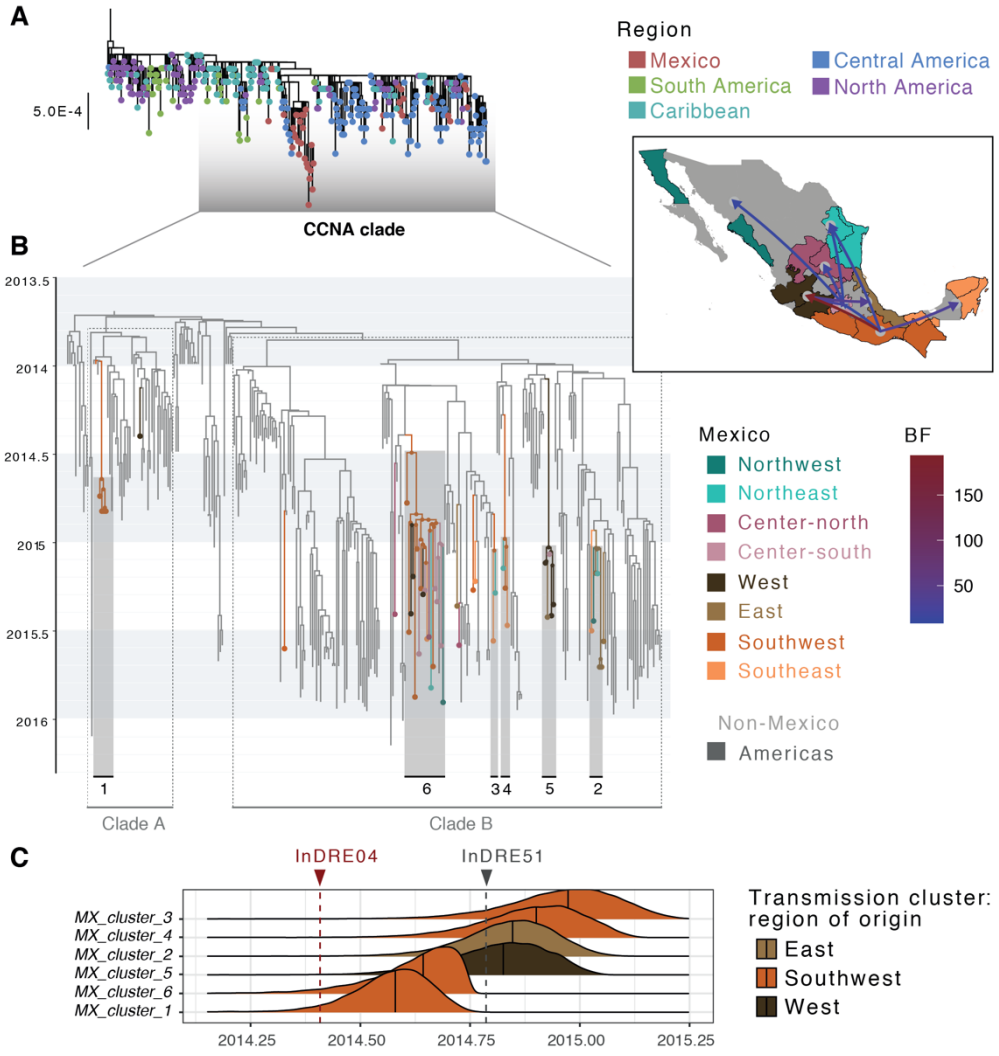

(A) ML phylogenetic tree of all CHIKV complete genome sequences from the Americas included in our analysis, with tips coloured by region of collection. ***(B)*** Time-calibrated phylogeographic analysis of the CHIKV CCNA. Tip and nodes for locations within Mexico and are coloured by region, with the main clusters identified numbered (1- 6). The map in the inset shows pairs of locations where transition rates significantly explain the phylogenetic diffusion process, as inferred under a BSSVS analysis. Only transition rates with a posterior probability (PP) > 0.5 are shown, coloured by Bayes Factor (BF). ***(C)*** Posterior probability densities for the TMRCAs of six CHIKV transmission clusters in Mexico. Median values for each distribution are indicated, with the distributions coloured by the most probable location of each MRCA. Collection dates for InDRE04 (the first sequence corresponding to a CHIKV imported case into Mexico, collected on 2014-05-30), and InDRE51 (the first confirmed autochthonous case within Mexico, collected on 2014-10-15) are shown in red and grey, respectively.

Consistent with previous observations, we estimate an earliest date for the root of the CCNA clade around mid-September 2013 (Median = 2013.6941, 95% HPD = 2013.5867 – 2013.7865 (**Fig 2A**) [62]. The most basal branches within the CCNA clade show early viral circulation predominantly within the Eastern Caribbean, suggesting multiple exportations into the Central Caribbean, South, Central and North America region. This includes two importations into Mexico, comprising the earliest sequence generated from the country (nDRE04. GenBank Accession KP795107 [36]), and a cluster of sequences from the southwestern state of Chiapas [64] (named here clade A; posterior probability, PP = 0.88) (**Fig 2B**). While sequences within clade A were generally no longer sampled after late 2014, a second well-supported clade (named here clade B; posterior probability, PP = 0.91) was identified. Before being introduced into Mexico, our results indicate that clade B had initially circulated within the Eastern Caribbean, but then shifted towards the Central Caribbean. Introductions into the USA occurred multiple times from both the Eastern and Central Caribbean regions, leading to subsequent introductions into Nicaragua (**Supplementary Information, Fig S4**). Within clade B, the Mexico genomes directly descend from sequences sampled from Nicaragua and the USA. Nonetheless, given the overrepresentation of sequences from the USA and Nicaragua (**Supplementary Information, Fig S1B**), it is likely that geographical sampling biases partially account for Nicaragua as inferred source location.

Reconstructing virus introduction events of CHIKV into Mexico revealed 13 clusters with MRCAs likely representing independent introductions from abroad, confirming previous observations on multiple independent introductions observed for CHIKV in Mexico [36–39]. In seven instances, Mexico sequences represent singleton events, denoting either returning travellers (as is the case with the aforementioned

304 InDRE04 sequence), or poorly sampled viral lineages. The remaining six genomes fall
305 within six well-supported clusters exclusive to Mexico (named here *MX_cluster_1* to
306 *MX_cluster_6*) (Fig 2A). For these clusters, the ancestral nodes (*i.e.* the most recent
307 common ancestor, MRCAs) were inferred to have emerged within the Southwest
308 ($PP_{MX\_cluster\_1}$ = 0.5619, $P_{Southwest}$ = 0.7649; $PP_{MX\_cluster\_3}$ = 0.9998, $P_{Southwest}$ = 0.662;
309 $PP_{MX\_cluster\_4}$ = 0.9462, $P_{Southwest}$ = 0.8362; $PP_{MX\_cluster\_6}$ = 0.9971, $P_{Southwest}$ = 0.9994),
310 in the East ($PP_{MX\_cluster\_2}$ = 0.5364, P_{East} = 0.6846) and in the West of the country
311 ($PP_{MX\_cluster\_5}$ = 0.5047, P_{West} = 0.9092) (**Fig 2B**). We identified three significant
312 transition rates across locations between the Americas and Mexico, namely into the
313 Southwest (BF = 5236.52; PP > 0.99), Centre-north (BF = 86.21; PP = 0.92) and West
314 (BF = 15.76; PP = 0.68) regions (Fig 2B and C). All MRCAs for these six Mexico
315 clusters dated between mid- and late-2014 (Table 3), with two of these (*MX_cluster_1*
316 and *MX_cluster_6*) predating the first autochthonous CHIKV case reported in the
317 country (represented by sequence InDRE51. GenBank accession number
318 KP795109). However, inferred dated for these MRCAs is later than the sampling date
319 of the earliest reported introduced CHIKV case in Mexico (InDRE04), with a known a
320 travel history into the Caribbean[36] (**Fig 2B**). The remaining clusters circulated in the
321 country since October 2014 (**Table 2**).

Table 2. Arbovirus clusters inferred from phylogeographic analyses

Virus		Mexico cluster	TMRCA		Ancestral location
			Median age	*95% HPD*	
CHIKV		*MX_cluster_1*	2014.57	2013.69 - 2014.74	Southwest
		MX_cluster_6	2014.64	2014.42 - 2014.75	Southwest
		MX_cluster_5	2014.83	2014.59 - 2015.01	East
		MX_cluster_2	2014.85	2014.62 - 2014.04	West
		MX_Cluster_4	2014.9	2014.6 - 2015.11	Southwest
		MX_cluster_3	2014.97	2014.72 - 2015.18	Southwest
DENV	DENV-2	*cluster_2*	1998.97	1997.35 - 2000.61	Southwest
	DENV-2	*cluster_1*	1999.51	1998.13 - 2000.79	Southwest
	DENV-1	*cluster_2*	2003.49	2002.31 - 2004.18	---
	DENV-1	*cluster_1*	2003.81	2001.63 - 2003.91	---
	DENV-1	*cluster_3*	2004.03	2003.01 - 2004.8	---
	DENV-2	*cluster_3*	2008.02	2007.15 - 2008.9	Southwest
	DENV-1	*cluster_4*	2009.35	2008.28 - 2010.2	---

Spatial dynamics of CHIKV across Central America and Mexico

The spread of CHIKV within Mexico was inferred to occur from the Southwest across the southern and central coastal regions of Mexico. We identified 14 supported transitions, with source regions predominantly represented by the West, Southwest and Centre-south (**Fig 2A** and **Supplementary Information, Table S3**). The *MX_cluster_1* makes up the largest transmission chain identified for CHIKV, circulating across 11 different states (Baja California Norte, Mexico state, Mexico City, Guerrero, Tamaulipas, San Luis Potosí, Quintana Roo, Jalisco, Morelos, Michoacán and Oaxaca) (Fig 2A). The second largest cluster (*MX_cluster_6),* corresponds to the earliest group of cases sampled from the state of Chiapas, thus is exclusive to the Southwest region [64]. Contrastingly, *MX_cluster_3 and MX_cluster_4* were only sampled from two regions each (comprising only 3 and 2 sequences, respectively), whilst *MX_cluster_5* circulated only across two regions in central Mexico (East and West). Finally, *MX_cluster_2* circulated across three regions in central and northern Mexico (East, Northeast and Northwest).

DENV genome data

Resulting from human and mosquito-derived DENV samples selected to represent a collection date between 2013 and 2017 and up to six states, we were able to generate 7 complete DENV-1 and 11 DENV-2 partial genomes (Table S1). For DENV-2, insufficient coverage for several genomic regions (including both UTRs) was obtained due to a partial failure during the multiplex PCR (genome regions that failed to amplify were masked with Ns (Supplementary Data 3). Nonetheless, successfully sequenced sites (5104/10177 bases, corresponding to ~50% of the genome length) encompassed partial ORFs for the capsid, envelope and glycoprotein (as well as various non-structural protein partial gene regions: NS1, NS2A, NS2B, NS3, NS4B and NS5). Such sequenced genome regions proved to have enough signal for further phylogenetic analyses, further highlighting the use of incomplete genome data for genomic epidemiologic-based phylodynamic inferrence [76]. Again, the newly generated genome data represent a considerable improvement of the spatiotemporal representation of DENV sequences from Mexico, which previously accounted only for sequences from 2012. Furthermore, genomes now represent two states with no previous data for DENV-1 (Chiapas and Veracruz), and four previously unrepresented states for DENV-2 (Colima, Jalisco, Morelos and Veracruz) (**Supplementary Information, Table S1**).

Epidemiological dynamics of DENV 1-2 in Mexico from 2013-2019

Analysis of DENV longitudinal epidemiological data from Mexico shows a clear virus seasonal pattern fluctuating between 2013 and 2019, with distinct trends across regions (**Supplementary Information, Fig S5**). During 2013, the Northeast, East and Southeast regions reported up to 3000 monthly cases at their respective peaks, with similar case numbers observed in the Northwest, West and Southwest regions, (with

366 monthly cases not exceeding 2500) (**Supplementary Information, Fig S5**). The
367 proportion of serotyped cases increased substantially between 2017 and 2018, when
368 the yearly cumulative number of cases was at the lowest (Fig S6). Most samples were
369 identified as DENV-1 or DENV-2, with a smaller portion of cases identified as DENV-
370 3 or co-infections with multiple serotypes (Fig 3). When contextualised alongside
371 previously reported data available for the proportion of DENV serotypes from 2000 to
372 2013 [77], it becomes clear that DENV-1 was practically absent from the country until
373 2004 and 2007, when it began to dominate over other viral serotypes. Since then,
374 DENV-1 and DENV-2 have been co-circulating showing epidemiological dominance
375 (**Fig 3A**). DENV serotype replacements have been widely described in Asia[78–80] and
376 South America[81], whilst a few studies of DENV in Mexico report frequent lineage
377 replacement events observed for distinct serotypes [40-42]. The periodic importations of
378 DENV into Mexico we detect throughout 2000-2010 may (partially) explain the shifting
379 dominance observed for specific DENV virus serotypes across time and space.

Fig 3. Epidemiological trends of different DENV serotypes in Mexico from 2013 to 2019

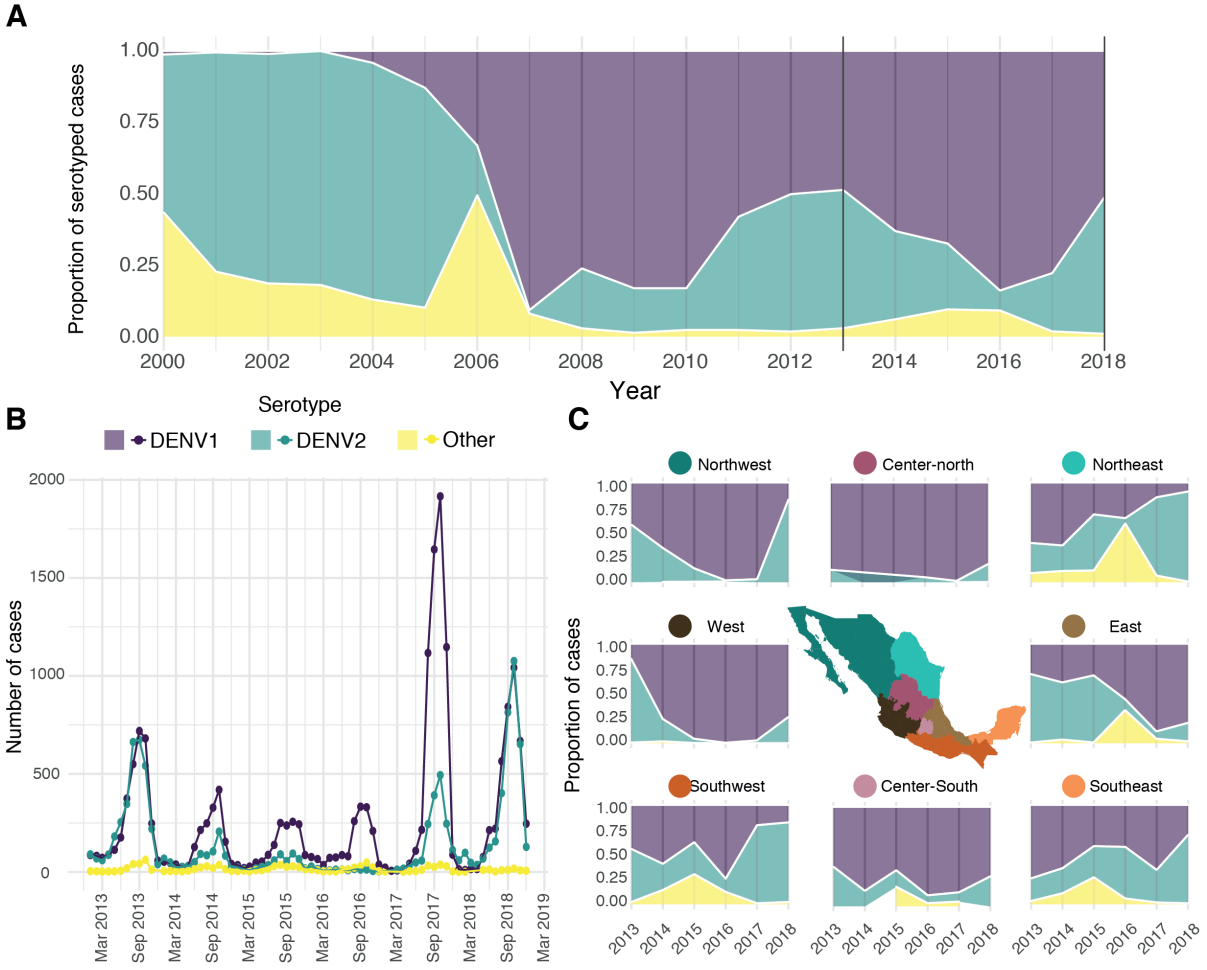

(A) The proportion of serotyped DENV cases between 2000 and 2018 in Mexico shown in reference to the total number of serotyped samples per year for all the country. Data provided by InDRE for this study is shown between the solid black lines (delimiting 2013 to 2018). Data from previous years was obtained from published sources[77]. The DENV-3 and DENV-4 serotypes together with potential co-infections (reported between 2013 and 2018) are grouped into the 'Other' category. ***(B)*** Monthly number of cases assigned to each DENV serotype in Mexico from 2013 to 2018. ***(C)*** Breakdown of serotype proportions in different geographic regions in Mexico between 2013 and 2019, relative to the total number of serotyped samples for each location.

For the DENV-1 data, a remarkable anomaly was noted: a peak in the number of DENV-1 cases was observed during 2017, whilst an equal proportion of both DENV-1 and DENV-2 serotypes was recorded at the same time (**Fig 3B**). This observation can be explained (at least partially) by the combination of an overall lower number of DENV cases in the country during this season, coupled with a highest rate of serotyping and case reporting from the Centre-north region of the country (**Supplementary Information, Fig S6**). Specifically, during 2017, the proportion of serotyped samples increased in relation to previous years (**Supplementary**

Information, Fig S7), with the Centre-north region serotyping ~95% of all cases. At the same time, the majority of cases typified as DENV-1 also came from the Centre-north, resulting in a biased epidemiological trend (**Supplementary Information, Figs S6-S8**). However, when breaking down epidemiological patterns per region, some common trends were observed (**Fig 3C**). Samples classified as 'other' DENV serotypes (neither DENV-1 or DENV-2) comprised the minority of the total serotyped cases, and were prominently observed in the East and Northeast region in 2016 (but were completely absent from the North-western region). The case proportion of DENV-2 in relation to DENV-1 decreased between 2013 and 2016 for most of the country, except for the Southeast region. Then, between 2016 and 2017, DENV-2 increased in frequency across the Northeast and Southwest regions, followed by the rest of the country (particularly in the West and Northwest) as later observed throughout 2018 (**Fig 3C**).

Evolutionary dynamics of DENV-1 and DENV-2 in Central America and Mexico

Compared to CHIKV, our phylogeographic analyses revealed that DENV-1 and DENV-2 display similar epidemiological and evolutionary trends. Specifically, for both DENV trees, sequences from Mexico and Nicaragua group together into single clades, along with a few sequences from Central American, North American and/or the Caribbean (for both cases, such clades are henceforth named here as CAM) (**Supplementary Information, Fig S9**). The CAM clades are comparable to the CCNA clade described for CHIKV, but were generally found to be more geographically constrained. For DENV-1, the CAM clade dates back to the early 2000s (median age MRCA $_{DENV\text{-}1\text{-}CAM}$ = 2000.5152, 95% HPD = 1997.8814 – 2002.2687), whilst for DENV-2 to the late 1990s (median age MRCA $_{DENV\text{-}2\text{-}CAM}$ = 1996.8204, 95% HPD = 1995.6215 – 1997.7913). Reconstructing the importation and spread patterns of DENV-1 and 2

in Mexico revealed that both CAM clades circulated predominantly in Nicaragua before they were periodically and independently introduced into Mexico. Five different introductions were identified for DENV-1, whilst three were detected for DENV-2. Nonetheless, as highlighted before, the overrepresentation of DENV genome sequences from Nicaragua, together with a limited reduced genome representation from other countries in the region, are likely to impact phylogeographic reconstructions (**Supplementary Information, Table S3**).

The sampling timespan for DENV viruses Mexico is mostly overlapping, with DENV-1 sequences collected between 2004 and 2017, and DENV-2 sequences collected between 2000 and 2019. The MRCAs for different clusters within the CAM clades show that both viruses circulated in the country since the late 1990s. For DENV-2, two clusters date back to 1999 and circulated until 2013, displaying a persistence of approximately 14 years. Consistently, for DENV-1, three clusters date back to the early 2000s, also circulating up to 2013. Later DENV introductions are associated with a cluster dating back to 2008 (for DENV-2), and another cluster dating back to 2009 (for DENV-1) (**Supplementary Information, Fig S9 and TableS3**).

Spatial dynamics of DENV-2 across Central America and Mexico

Whilst DENV-2 genomes have been sampled extensively across southern and central Mexico, the geographical distribution for DENV-1 genomes is mostly limited to the Southeast region. Thus, DENV-2 is used here to illustrate general DENV spread dynamics across the country (**Fig 4**).

448 **Fig 4. Time-scaled analysis for DENV-2 in Mexico**
449

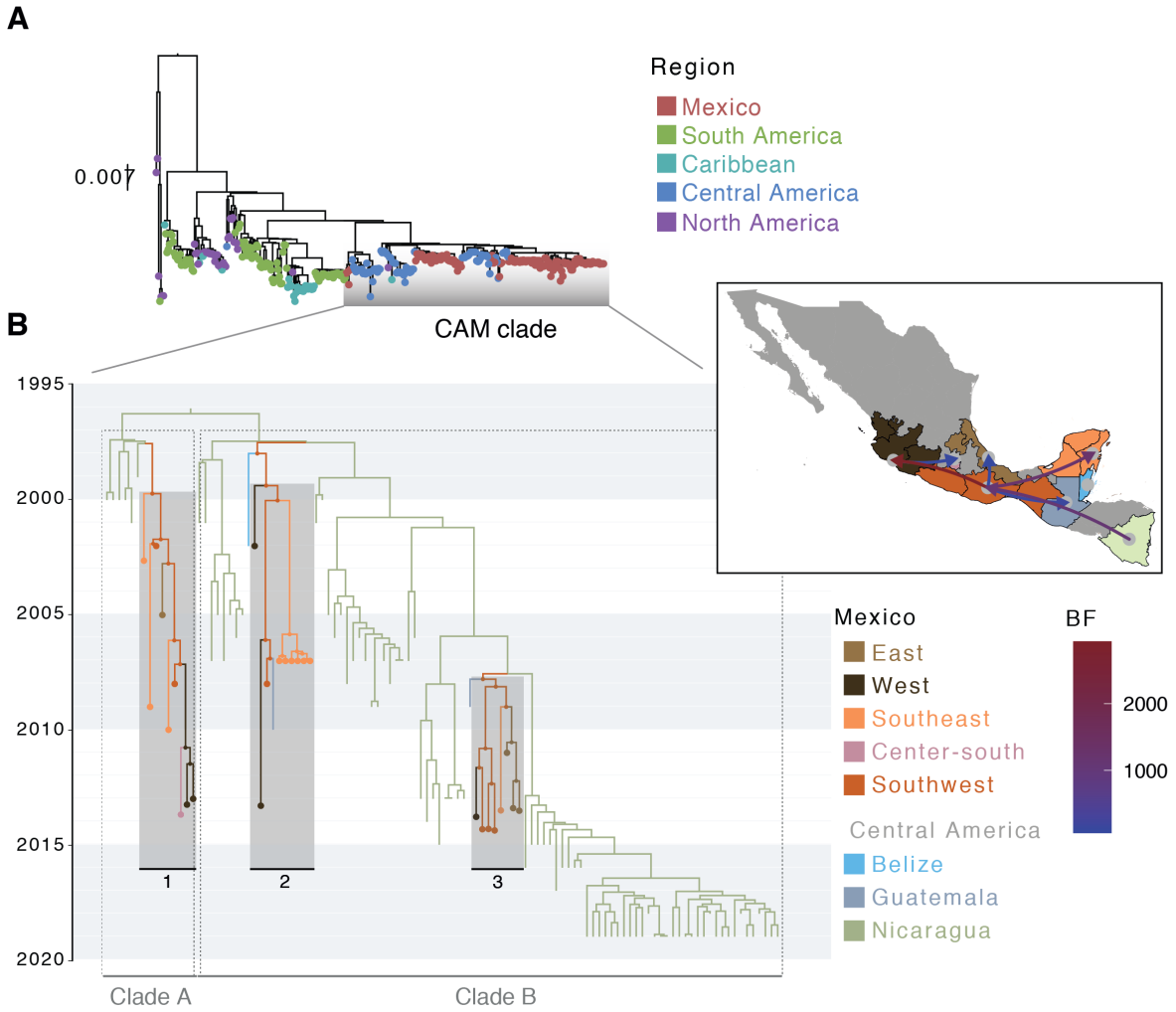

450
451 ***(A)*** ML phylogenetic tree for DENV-2 in the Americas, with tips coloured according to the geographic
452 region of collection. ***(B)*** Time-calibrated phylogeographic analysis for the DENV-2 CAM lineage, with
453 the MCC tree displaying different sampling locations for Mexico. Tip and nodes shapes are included for
454 locations within Mexico, coloured by region. Distinct clades identified within the CAM lineage are
455 designated as Clade A (including one cluster from Mexico) and Clade B (including two clusters from
456 Mexico). The map in the inset shows pairs of locations for which transition rates were inferred to be
457 significant under a BSSVS analysis. Only transition rates with a posterior probability (PP) > 0.5 are
458 shown, coloured by Bayes Factor (BF).
459

460 Phylogeographic reconstruction shows that the three DENV-2 clusters are likely to
461 have originated in the Southwest of the country, further spreading towards the East
462 and West coasts, and into the Yucatán peninsula (**Fig 4**). Movements observed
463 between Nicaragua and the Southwest of the country support the importation events
464 inferred for DENV-2 into Mexico (BF = 1124.01, PP = 0.99), with subsequent spread
465 into other states towards the North. Within Mexico, viral movements from the

Southwest into the West (BF = 2929.53, PP > 0.99), Southeast (BF = 1270.88, PP > 0.99) and East (BF = 56.08, PP = 0.90) were inferred as significant. Movements from the West to the Centre-south region (namely the state of Morelos) were also significant (BF = 83.25, PP = 0.93), as well as across border movements from south into Guatemala (BF = 134.65, PP = 0.96).

Given the longitudinal collection of DENV-1 and DENV-2 epidemiological data for almost two decades within the country, changes in the population size over time can be estimated by integrating genomic data under a Bayesian Skyline plot (BSP) (see Methods section: *Time-calibrated phylogeographic analyses).* The BSPs for both the DENV-1 and DENV-2 CAM lineages show different periods of time representing viral population growth (suggesting an increase in the number of new cases in Mexico): 2005-2007 and 2011-2013 for DENV-1, and 2017-2018 for DENV-2 (**Supplementary Information, Fig S10**). These periods coincide with a relative increase in cases associated to each specific serotype: for DENV-1 observed between 2005-2007, and for DENV-2 between 2017-2018. For DENV-2, the population growth period identified between 2011-2013 overlaps with a decrease in the serotype's proportion relative to DENV-1, followed a subsequent increase observed between 2013-2016 (Fig S10). Overall, no clear pattern between the BSP and serotype frequencies was evident.

DISCUSSION

In order to investigate convergence within the epidemiological and evolutionary dynamics of CHIKV, DENV-1 and DENV-2 viruses circulating in Mexico, we generated complete and partial virus genomes, and analysed them together with genome and epidemiological data from the Americas collected over almost two decades. We find important similarities represented by multiple virus introduction events into the country

492 derived from lineages predominantly sampled from the Caribbean and Central
493 America. These three arboviruses also share comparable spatiotemporal
494 transmission trends, in which the Southwest region of the country seems to have
495 played a pivotal role in virus seeding and spread across Mexico.

496 The phylogeographic analysis we present for DENV-2 (representing general
497 spatial dynamics of DENV in Mexico) revealed multiple virus importations into the
498 country leading to extended transmission chains, with a most probable within-country
499 location for viral introductions determined to be the state of Chiapas. Comprising a
500 better spatial and temporal sampling within a single epidemic, the spatial diffusion
501 pattern observed for CHIKV was found to be comparable, with most transmission
502 clusters displaying the same inferred ancestral location. Of notice, in an independent
503 study by Thézé et al. 2018 [76], a similar trend was also described for ZIKV in Mexico,
504 again showing a most likely virus introduction into Chiapas, with subsequent spread
505 towards the north of the country. Our results further support for an unbiased inference,
506 as viral genomes sampled from this region were not particularly overrepresented
507 within our datasets. However, an extended genomic representation within the country
508 could contribute to portray a more complete panorama of arboviral spread patterns at
509 a higher resolution (*i.e.*, across states).

510 Within a global context, southern tropical regions are known to provide the ideal
511 ecological conditions related to vector competence and establishment, and thus have
512 been historically associated with arboviral outbreaks [6,80]. There is further evidence that
513 arboviruses display seeding and spread trends that derive from high-prevalence
514 areas, commonly located within southern regions in the Americas [82]. In this light,
515 longitudinal epidemiological case data derived from arbovirus epidemics in Mexico
516 support for the southern tropical region of the country as an important hub for viral
517 transmission [76], regardless of putative systematic biases towards an increased

518 arbovirus case detection given an intensified surveillance within the area. Thus, the
519 independent association of the Southwestern region of Mexico as a source location
520 for the introduction of DENV, CHIKV and ZIKV, provides strong evidence for
521 convergence in the spatial dynamics of both seasonal and emerging *Aedes*-borne
522 arboviruses circulating within the country.

523 The spread of arboviruses in the Americas is largely known to be driven by
524 human mobility patterns [6]. Our results suggest that arboviral importation and spread
525 in Mexico have been driven to some extent by human movements, as has been shown
526 for other countries [6,80]. In this context, the arboviral diffusion patterns we observe are
527 potentially linked to human movements across borders, particularly following land-
528 based unregulated migration routes from central America into Mexico and towards the
529 USA [88,89] [85,86,87]. Thus, incorporating migration-informed genome sequencing into
530 disease surveillance could help inform on arbovirus control, as human mobility is
531 expected to potentially increase due to changing political and socio-economic factors
532 throughout the region. Nonetheless, whilst human mobility is an important determinant
533 for arbovirus epidemics, viral spread is very much shaped by other climatic, ecological
534 and immunological factors[1,2, 11–13].

535 As an example, the ability of arboviruses to establish a sustained or seasonal
536 transmission in a recipient geographical area, depends on climatic and ecological
537 condition, as well as the viral capacity to persistently infect the vector population. In
538 Mexico, arbovirus persistence is reflected by somewhat independent epidemiological
539 trends observed across distinct regions of the country, exemplified by the Yucatan
540 peninsula, that compared to other regions of Mexico, showed a unique epidemiological
541 trend during the late CHIKV peak in 2015. Thus, exploring arbovirus spatial diffusion
542 patterns across different different scales can only be achieved through comprehensive

543 approaches that integrate multiple sourced information (including social, ecological,
544 genomic and epidemiological data).

545 Predicting spatial spread patterns for arboviruses could play an important role
546 in the design of surveillance programs and public health interventions, such as the
547 implementation of vaccine trials. In this scenario, previous immunity within the host
548 population is an important covariate to consider when interpreting our results. In this
549 sense, it is not a surprise that the Southwest of the country (displaying the ideal
550 ecological suitability for vectors, coupled with a higher probability of new arboviral
551 importations that may result in extended transmission chains) shows the highest
552 seroprevalence for DENV[13]. Congruently, other regions in Mexico showing
553 subsequent domestic virus importations from the Southwest (such as the West and
554 Southeast), also show a high seroprevalence[90,91]. Thus, our results may inform on
555 suitable locations for vaccine trials, where high numbers of new cases are required to
556 achieve targets of efficacy promptly [92].

557 Limitations of our study include biases for inferred source locations for arboviral
558 introductions from abroad, likely to be impacted by differences in genomic surveillance
559 efforts across countries within the same region. In this light, multiple viral introductions
560 were inferred from Nicaragua into the country, indicating that arbovirus epidemics in
561 Mexico are likely to be affected by neighbouring countries [83]. Nevertheless, whilst
562 Nicaragua features a considerable genomic representation in Latin America [47,48], other
563 countries in central America (such as Belize, Guatemala, Honduras and El Salvador)
564 have limited publicly available arbovirus genome data, and thus virus introductions
565 from neighbouring countries could not be inferred. Further limitations comprise
566 sampling gaps that can bias the inference of ancestral locations at nodes [84], reflected
567 by long branches separating the clusters identified (indicative of long cryptic circulation
568 periods, or an unsampled virus genetic diversity) that may result in uncertainty in date

569 estimates derived from time-calibrated phylogenies. Thus, only an enhanced spatial
570 and temporal virus genome sampling and sequencing across bordering countries will
571 enable a more detailed exploration of arboviral dynamics in the region.

572 Multiple tools have been developed to guide the implementation of
573 interventions to control the transmission of arboviral diseases [82,83,93]. Our results add
574 to the current knowledge of arboviral dynamics in Mexico, highlighting the potential
575 predictability of spatial invasion dynamics. Further incorporating our results into
576 current epidemiological and spatial models may enhance the accuracy of current risk
577 maps for established and emerging arboviruses in Mexico and Central America.
578 Finally, the key role of neighbouring South American countries in the development of
579 arboviral epidemics in Mexico, and of the country's southern border in the spread of
580 arboviruses at national scale, prompts the need to better understand the role of
581 anthropogenic factors in the transmission dynamics of viral pathogens, particularly
582 concerning the effects of land-based migration. Our study further pinpoints on how
583 joint efforts between public health and academic institutions can foster genomic
584 epidemiology-based surveillance strategies applied to the developing world.

SUPPORTING INFORMATION CAPTIONS

- Supplementary Text 1: Retrospective on the arbovirus epidemics in the Americas and epidemiological surveillance in Mexico
- Fig S1. CHIKV epidemiological and genomic surveillance trends in the Americas
- Fig S2. Complete CHIKV genome sequences versus total cases reported to PAHO per country
- Fig S3. CHIKV epidemiological trends across Mexico between 2016 and 2018
- Fig S4. Phylogenetic analyses of CHIKV in the Americas.
- Fig S5. DENV epidemiological trends across Mexico between 2016 and 2018
- Fig S6. Serotyping representation for DENV across regions in Mexico
- Fig S7. DENV serotyping efficacy across time in different Mexico regions
- Fig S8. DENV-1 and DENV-2 case numbers across Mexico regions
- Fig S9. Phylogenetic analyses of DENV-1 and DENV-2 in the Americas
- Fig S10. Bayesian Skyline plot of the CAM DENV-1 and DENV-2 lineages
- Table S1. Genome sequences generated in this study
- Table S2. PAHO regions
- Table S3. BSSVS results for CHIKV
- Table S4. BSSVS results for DENV-2

DATA AVAILABILITY

Virus sequences generated in this study are provided as alignments in Supplementary Data 1 (CHIKV), 2 (DENV-1) and 3 (DENV-2). GenBank Accession numbers for the publicly available sequences used in this study are listed in the Supplementary Data 4.

AUTHOR CONTRIBUTIONS

BG performed research and analysed data. CDDS and SB analysed data. Together with member of the 'Technological development and molecular research unit' and the 'National Arbovirus Reference Laboratory' (ERMC, APRM, FGA, MLTR, AAR, CWA), BG and CDDS carried out sample selection and laboratory work, coordinated by ERG, ILM, JADQ and MVP at InDRE and by MEZ. SCH, JT, NF and OP contributed to revising the methodological approach and to overcome technical aspects of the sequencing. ARS, MK, and MEZ contributed to the initial experimental design of the study. MEZ and MK supervised and coordinated data analysis. BG and MEZ wrote the manuscript, with contributions and comments from all authors.

COMPETING INTERESTS

The authors declare no competing interests.

ACKNOWLEDGEMENTS

We would like to thank the personnel at the National Institute for Epidemiological Diagnosis and Reference (Instituto de Diagnóstico y Referencia Epidemiológicos "Dr. Manuel Martínez Báez" – InDRE, Secretaría de Salud, Mexico- WHO Collaborating Center in Arbovirus), for their support in sharing samples and data from the 'National Arbovirus Reference Laboratory', and for contributing to the molecular biology and sequencing laboratory work at the 'Technological development and molecular research unit'. We thank Dr. Santa Elizabeth Ceballos Liceaga, Head of the Epidemiological Surveillance of Communicable Diseases at the 'General Directorate of Epidemiology' (DGE, Secretaría de Salud, Mexico) for her support in sharing epidemiological data. We also thank Dr. Lorena Preciado-Llanes from the Jenner Institute at the University of Oxford for her assistance with funds management and

reporting. We would also like to thank Seth Flaxman and Simon Dellicour for their input and insightful discussions on this manuscript. This research was funded by United Kingdom Research & Innovation office and the Department of Health and Social Care using UK Aid funding, managed by the BBSRC/EPSRC/NIHR 971557 (to A.R.S). The views expressed in this publication are those of the author(s) and not necessarily those of the Department of Health and Social Care. The project was further funded by the John Fell OUP Research Fund Award 0008724 (Project ATD00390 to MEZ and MUGK). SCH is supported by a Wellcome Trust Sir Henry Wellcome Postdoctoral Fellowship (220414/Z/20/Z). OGP and MUGK acknowledges support of the Oxford Martin School. MUGK and JT acknowledge support from the European Union Horizon 2020 project MOOD (#874850). MEZ is supported by Leverhulme Trust ECR Fellowship (ECF-2019-542).

ETHICS STATEMENT

We declare that under the authority of the ethics committee “Comite de etica e investigacion del ICSa – UAEH” (Instituto de Ciencias de la Salud/Universidad Autónoma del Estado de Hidalgo, Mexico), our study has been granted ethical approval registered under the following number: ICSa 57/2023 (signed by the president Dra. Itzia Maria Cazares Palacios on March 6th 2023).

REFERENCES

1. Oki, M. & Yamamoto, T. Climate Change, Population Immunity, and Hyperendemicity in the Transmission Threshold of Dengue. *PLoS One* **7**, (2012).
2. Redding, D. W. *et al.* Geographical drivers and climate-linked dynamics of Lassa fever in Nigeria. *Nat Commun* **12**, 1–10 (2021).
3. Dudas, G., Carvalho, L. M., Rambaut, A. & Bedford, T. MERS-CoV spillover at the camel-human interface. *Elife* **7**, 1–23 (2018).
4. Kilpatrick, A. M. & Randolph, S. E. Drivers, dynamics, and control of emerging vector-borne zoonotic diseases. *The Lancet* **380**, 1946–1955 (2012).
5. Faria, N. R. *et al.* Genomic and epidemiological monitoring of yellow fever virus transmission potential. *bioRxiv* **899**, 894–899 (2018).
6. Allicock, O. M. *et al.* Determinants of dengue virus dispersal in the americas. *Virus Evol* **6**, 1–13 (2020).
7. Reiter, P. *et al.* Texas lifestyle limits transmission of dengue virus. *Emerg Infect Dis* **9**, 86–89 (2003).
8. Faria, N. R. *et al.* Zika virus in the Americas: Early epidemiological and genetic findings. *Science (1979)* **352**, 345–349 (2016).
9. Kraemer, M. U. G. *et al.* The effect of human mobility and control measures on the COVID-19 epidemic in China. *Science (1979)* **368**, 493–497 (2020).
10. Churakov, M., Villabona-Arenas, C. J., Kraemer, M. U. G., Salje, H. & Cauchemez, S. Spatio-temporal dynamics of dengue in Brazil: Seasonal travelling waves and determinants of regional synchrony. *PLoS Negl Trop Dis* **13**, 1–13 (2019).
11. Ferguson, N., Anderson, R. & Gupta, S. The effect of antibody-dependent enhancement on the transmission dynamics and persistence of multiple-strain pathogens. *Proc Natl Acad Sci U S A* **96**, 790–794 (1999).
12. Salje, H. *et al.* Dengue diversity across spatial and temporal scales: Local structure and the effect of host population size. *Science (1979)* **355**, 1302–1306 (2017).
13. Rodríguez-Barraquer, I., Salje, H. & Cummings, D. A. T. Opportunities for improved surveillance and control of infectious diseases from age-specific case data. *Elife* **8**, e45474 (2019).
14. Robert, M. A., Christofferson, R. C., Weber, P. D. & Wearing, H. J. Temperature impacts on dengue emergence in the United States : Investigating the role of seasonality and climate change. *Epidemics* **28**, 100344 (2019).
15. Akhmetzhanov, A. R., Asai, Y. & Nishiura, H. Quantifying the seasonal drivers of transmission for Lassa fever in Nigeria. (2019).
16. George, D. B. *et al.* Host and viral ecology determine bat rabies seasonality and maintenance. (2011) doi:10.1073/pnas.1010875108/-/DCSupplemental.www.pnas.org/cgi/doi/10.1073/pnas.1010875108.
17. Xiao, Y. *et al.* Modelling the Effects of Seasonality and Socioeconomic Impact on the Transmission of Rift Valley Fever Virus. **9**, (2015).
18. Gubler, D. J., Vasilakis, N. & Musso, D. History and Emergence of Zika Virus. **216**, 860–867 (2017).
19. Njenga, M. K. *et al.* Tracking epidemic Chikungunya virus into the Indian Ocean from East Africa. 2754–2760 (2008) doi:10.1099/vir.0.2008/005413-0.
20. Morris, T. E. Reemergence of Chikungunya virus. *J Virol* **88**, 11644–11647 (2014).
21. Muyembe-Tamfum, J. J. *et al.* Ebola virus outbreaks in Africa: Past and present. *Onderstepoort Journal of Veterinary Research* **79**, 1–8 (2012).
22. Daszak, P. *et al.* The emergence of Nipah and Hendra virus: Pathogen dynamics across a wildlife-livestockhuman continuum. in *Disease Ecology: Community Structure and Pathogen Dynamics* 186–201 (2007). doi:10.1093/acprof:oso/9780198567080.003.0013.
23. Borchering, R. K. *et al.* Impacts of Zika emergence in Latin America on endemic dengue transmission. *Nat Commun* **10**, (2019).
24. Ribeiro, G. S. *et al.* Does immunity after Zika virus infection cross-protect against dengue? *Lancet Glob Health* **6**, e140–e141 (2018).
25. Mugabe, V. A. *et al.* Changes in the dynamics of dengue incidence in South and Central America are possibly due to cross-population immunity after Zika virus epidemics. *Tropical Medicine and International Health* **26**, 272–280 (2021).
26. Carey, D. E. Chikungunya and dengue: A case of mistaken identity? *J Hist Med Allied Sci* **26**, 243–262 (1971).

27. Gould, E., Pettersson, J., Higgs, S., Charrel, R. & Lamballerie, X. De. Emerging arboviruses : Why today ? **4**, 1–13 (2017).
28. Weaver, S. C. Arrival of Chikungunya Virus in the New World: Prospects for Spread and Impact on Public Health. *PLoS Negl Trop Dis* **8**, 6–9 (2014).
29. Allicock, O. M. *et al.* Phylogeography and population dynamics of dengue viruses in the Americas. *Mol Biol Evol* **29**, 1533–1543 (2012).
30. Gubler, D. J. Dengue and Dengue Hemorrhagic Fever. **11**, 480–496 (1998).
31. InDRE, I. de D. y R. E. "Dr. M. M. B. *Lineamientos para la vigilancia por laboratorio del dengue y otras arbovirosis*. (2021).
32. Nava-Frías, M., Searcy-Pavía, R. E., Juárez-Contreras, C. A. & Valencia-Bautista, A. Chikungunya fever: Current status in Mexico. *Bol Med Hosp Infant Mex* **73**, 67–74 (2016).
33. Montesano-Castellanos, R. & Ruiz-Matus, C. Vigilancia epidemiológica del dengue en México. *Salud Publica Mex* **370**, S64–S76 (1995).
34. Briseño-García, B. *et al.* Potential Risk for Dengue Hemorrhagic Fever: The Isolation of Serotype Dengue-3 in Mexico. *Emerg Infect Dis* **2**, 133–135 (1996).
35. Fernandes-Matano, L. *et al.* Impact of the introduction of chikungunya and zika viruses on the incidence of dengue in endemic zones of mexico. *PLoS Negl Trop Dis* **15**, 1–16 (2021).
36. Díaz-Quiñonez, J. A. *et al.* Complete genome sequences of chikungunya virus strains isolated in Mexico: First detection of imported and autochthonous cases. *Genome Announc* **3**, (2015).
37. Laredo-Tiscareño, S. V. *et al.* Arbovirus surveillance near the Mexico-U.S. Border: Isolation and sequence analysis of chikungunya virus from patients with dengue-like symptoms in reynosa, tamaulipas. *American Journal of Tropical Medicine and Hygiene* **99**, 191–194 (2018).
38. Muñoz-Medina, J. E. *et al.* Evolutionary analysis of the Chikungunya virus epidemic in Mexico reveals intra-host mutational hotspots in the E1 protein. *PLoS One* **13**, 1–18 (2018).
39. Galán-Huerta, K. A. *et al.* Molecular and clinical characterization of Chikungunya virus infections in Southeast Mexico. *Viruses* **10**, 1–18 (2018).
40. Carrillo-Valenzo, E. *et al.* Evolution of dengue virus in Mexico is characterized by frequent lineage replacement. *Arch Virol* **155**, 1401–1412 (2010).
41. Hernández-García, E. *et al.* Epidemiological implications of the genetic diversification of dengue virus (DENV) serotypes and genotypes in Mexico. *Infection, Genetics and Evolution* **84**, 104391 (2020).
42. Zárate, S. *et al.* Complete genome of DENV2 isolated from mosquitoes in Mexico. *Infection, Genetics and Evolution* **71**, 98–107 (2019).
43. Hill, S. C. *et al.* Early Genomic Detection of Cosmopolitan Genotype of Dengue Virus Serotype 2, Angola, 2018. *Emerg Infect Dis* **25**, 784–787 (2019).
44. Naveca, F. G. *et al.* Genomic, epidemiological and digital surveillance of Chikungunya virus in the Brazilian Amazon. *PLoS Negl Trop Dis* **13**, 1–21 (2018).
45. Quick, J. *et al.* Multiplex PCR method for MinION and Illumina sequencing of Zika and other virus genomes directly from clinical samples. **12**, (2017).
46. Id, V. F. *et al.* A computational method for the identification of Dengue , Zika and Chikungunya virus species and genotypes. 1–15 (2019).
47. Edgerton, S. V. *et al.* Evolution and epidemiologic dynamics of dengue virus in Nicaragua during the emergence of chikungunya and Zika viruses. *Infection, Genetics and Evolution* **92**, 104680 (2021).
48. Balmaseda, A. *et al.* Trends in patterns of dengue transmission over four years of a pediatric cohort study in Nicaragua. *J Infect Dis.* **201**, 5–14 (2010).
49. Katoh, K. & Standley, D. M. MAFFT multiple sequence alignment software version 7: Improvements in performance and usability. *Mol Biol Evol* **30**, 772–780 (2013).
50. Minh, B. Q. *et al.* IQ-TREE 2: New Models and Efficient Methods for Phylogenetic Inference in the Genomic Era. *Mol Biol Evol* **37**, 1530–1534 (2020).
51. Guindon, S. *et al.* New algorithms and methods to estimate maximum-likelihood phylogenies: Assessing the performance of PhyML 3.0. *Syst Biol* **59**, 307–321 (2010).
52. Rambaut, A., Lam, T. T., Carvalho, L. M. & Oliver, G. Exploring the temporal structure of heterochronous sequences using TempEst (formerly Path-O-Gen). **2**, 1–7 (2016).
53. Suchard, M. A. *et al.* Bayesian phylogenetic and phylodynamic data integration using BEAST 1 . 10. **4**, 1–5 (2018).
54. Minin, V. N., Bloomquist, E. W. & Suchard, M. A. Smooth Skyride through a Rough Skyline : Bayesian Coalescent-Based Inference of Population Dynamics. (2000) doi:10.1093/molbev/msn090.
55. Drummond, A. J., Ho, S. Y. W., Phillips, M. J. & Rambaut, A. Relaxed phylogenetics and dating with confidence. *PLoS Biol* **4**, 699–710 (2006).

56. Ferreira, M. A. R. & Suchard, M. A. Bayesian analysis of elapsed times in continuous-time Markov chains. **36**, 355–368 (2008).
57. Rambaut, A., Drummond, A. J., Xie, D., Baele, G. & Suchard, M. A. Posterior summarization in Bayesian phylogenetics using Tracer 1.7. *Syst Biol* **67**, 901–904 (2018).
58. Drummond, A. J., Rambaut, A., Shapiro, B. & Pybus, O. G. Bayesian coalescent inference of past population dynamics from molecular sequences. *Mol Biol Evol* **22**, 1185–1192 (2005).
59. Lemey, P., Rambaut, A., Drummond, A. J. & Suchard, M. A. Bayesian phylogeography finds its roots. *PLoS Comput Biol* **5**, (2009).
60. Kass, R. E. & Raftery, A. E. Bayes Factors. *J Am Stat Assoc* **90**, 773–795 (1995).
61. Minin, V. N. & Suchard, M. A. Counting labeled transitions in continuous-time Markov models of evolution. *J Math Biol* **56**, 391–412 (2008).
62. Sahadeo, N. S. D. *et al.* Understanding the evolution and spread of chikungunya virus in the Americas using complete genome sequences. *Virus Evol* **3**, 1–10 (2017).
63. Nunes, M. R. T. *et al.* Emergence and potential for spread of Chikungunya virus in Brazil. *BMC Med* **13**, (2015).
64. Kautz, T. F. *et al.* Chikungunya Virus as Cause of Febrile Illness Outbreak, Chiapas, Mexico, 2014. *Emerg Infect Dis* **21**, 2070–2073 (2015).
65. Cunha, M. S. *et al.* Chikungunya Virus: An Emergent Arbovirus to the South American Continent and a Continuous Threat to the World. *Front Microbiol* **11**, (2020).
66. Sahadeo, N. *et al.* Molecular Characterisation of Chikungunya Virus Infections in Trinidad and Comparison of Clinical and Laboratory Features with Dengue and Other Acute Febrile Cases. *PLoS Negl Trop Dis* **9**, 1–18 (2015).
67. Wang, C. *et al.* Chikungunya virus sequences across the first epidemic in Nicaragua, 2014-2015. *American Journal of Tropical Medicine and Hygiene* **94**, 400–403 (2016).
68. Carrera, J. P. *et al.* Unusual pattern of chikungunya virus epidemic in the Americas, the Panamanian experience. *PLoS Negl Trop Dis* **11**, 1–23 (2017).
69. Khan, K. *et al.* Assessing the Origin of and Potential for International Spread of Chikungunya Virus from the Caribbean. *PLoS Curr* 4055609 (2014) doi:10.1371/currents.outbreaks.2134a0a7bf37fd8d388181539fea2da5.
70. Berry, I. M. *et al.* The origins of dengue and chikungunya viruses in Ecuador following increased migration from Venezuela and Colombia. **8**, 1–12 (2020).
71. Camacho, D. *et al.* Asian genotype of Chikungunya virus circulating in Venezuela during 2014. *Acta Trop* **174**, 88–90 (2017).
72. Leparc-Goffart, I., Nougairede, A., Cassadou, S., Prat, C. & De Lamballerie, X. Chikungunya in the Americas. *The Lancet* **383**, 514 (2014).
73. Xavier, J. *et al.* Circulation of chikungunya virus East/Central/ South African lineage in Rio de Janeiro, Brazil. *PLoS One* **14**, 1–14 (2019).
74. Lanciotti, R. S. & Valadere, A. M. Transcontinental movement of Asian Genotype Chikungunya virus. *Emerg Infect Dis* **20**, 1400–1402 (2014).
75. Nasci, R. S. Movement of Chikungunya virus into the Western Hemisphere. *Emerg Infect Dis* **20**, 1394–1395 (2014).
76. Thézé, J. *et al.* Genomic Epidemiology Reconstructs the Introduction and Spread of Zika Virus in Central America and Mexico. *Cell Host Microbe* **23**, 855-864.e7 (2018).
77. Dantés, H. G., Farfán-Ale, J. A. & Sarti, E. Epidemiological Trends of Dengue Disease in Mexico (2000–2011): A Systematic Literature Search and Analysis. *PLoS Negl Trop Dis* **8**, (2014).
78. Zhang, C. *et al.* Clade Replacements in Dengue Virus Serotypes 1 and 3 Are Associated with Changing Serotype Prevalence †. **79**, 15123–15130 (2005).
79. Adams, B. *et al.* Cross-protective immunity can account for the alternating epidemic pattern of dengue virus serotypes circulating in Bangkok. (2006).
80. Li, N. *et al.* The Lancet Regional Health - Western Pacific Assessing the impact of COVID-19 border restrictions on dengue transmission in Yunnan Province , China : an observational epidemiological and phylogenetic analysis. *Lancet Reg Health West Pac* **14**, 100259 (2021).
81. Faria, N. R. *et al.* Genomic and epidemiological characterisation of a dengue virus outbreak among blood donors in Brazil. *Sci Rep* **7**, 1–12 (2017).
82. Dzul-Manzanilla, F. *et al.* Identifying urban hotspots of dengue, chikungunya, and Zika transmission in Mexico to support risk stratification efforts: a spatial analysis. *Lancet Planet Health* **5**, e277–e285 (2021).
83. Kraemer, M. U. G. *et al.* Past and future spread of the arbovirus vectors Aedes aegypti and Aedes albopictus. *Nat Microbiol* **4**, 854–863 (2019).
84. De Maio, N., Wu, C. H., O'Reilly, K. M. & Wilson, D. New Routes to Phylogeography: A Bayesian Structured Coalescent Approximation. *PLoS Genet* **11**, 1–22 (2015).

85. Riosmena, F. & Massey, D. S. Pathways to El Norte : Origins , Destinations , and Characteristics of Mexican Migrants to the United States 1. **46**, 3–36 (2012).
86. Massey, D. S. Patterns of U . S . Migration from Mexico , the Caribbean , and Central America. **2**, 5–39 (2003).
87. Lemey, P. *et al.* Unifying Viral Genetics and Human Transportation Data to Predict the Global Transmission Dynamics of Human Influenza H3N2. *PLoS Pathog* **10**, (2014).
88. Global Migration Data Analysis Centre. Migration data in central America. *Migration data portal*.
89. París-Pombo, M. D. Trayectos peligrosos: Inseguridad y movilidad humana en México. *Papeles Poblac* **22**, 145–172 (2016).
90. Amaya-Larios, I. Y. *et al.* Seroprevalence of neutralizing antibodies against dengue virus in two localities in the state of Morelos, Mexico. *American Journal of Tropical Medicine and Hygiene* **91**, 1057–1065 (2014).
91. Hladish, T. J. *et al.* Projected Impact of Dengue Vaccination in Yucatán, Mexico. *PLoS Negl Trop Dis* **10**, 1–19 (2016).
92. Farrington, C. P. & Miller, E. Vaccine Trials. **17**, (2001).
93. Muñoz, G. *et al.* AeDES: a next-generation monitoring and forecasting system for environmental suitability of Aedes-borne disease transmission. *Sci Rep* **10**, 1–13 (2020).
94. Mowatt, L. & Jackson, S. T. Chikungunya in the Caribbean: An Epidemic in the Making. *Infect Dis Ther* **3**, 63–68 (2014).
95. Johansson, M. A. Chikungunya on the move. *Trends Parasitol* **31**, 43–45 (2015).
96. de Oliveira, E. C. *et al.* Short report: Introduction of chikungunya virus ecsa genotype into the brazilian midwest and its dispersion through the americas. *PLoS Negl Trop Dis* **15**, 1–10 (2021).
97. Johansson, M. A., Powers, A. M., Pesik, N., Cohen, N. J. & Erin Staples, J. Nowcasting the spread of Chikungunya Virus in the Americas. *PLoS One* **9**, (2014).
98. Escobar, L. E., Qiao, H. & Peterson, A. T. Forecasting Chikungunya spread in the Americas via data-driven empirical approaches. *Parasit Vectors* **9**, 1–12 (2016).
99. Nunez-Avellaneda, D. *et al.* Chikungunya in Guerrero, Mexico, 2019 and Evidence of Gross Underreporting in the Region. *Am J Trop Med Hyg* **105**, 1281–1284 (2021).
100. Pinheiro, F. & Nelson, M. Re-Emergence of Dengue and Emergence of Dengue Haemorrhagic Fever in the Americas. *Dengue Bull* **21**, 1–6 (1997).
101. Gordon, A. *et al.* The Nicaraguan Pediatric Dengue Cohort Study : Incidence of Inapparent and Symptomatic Dengue Virus. **7**, 2004–2010 (2013).
102. Tami, A., Lizarazo, E. F. & Grillet, M. E. ENSO-driven climate variability promotes periodic major outbreaks of dengue in Venezuela. *Sci Rep* 1–11 (2018) doi:10.1038/s41598-018-24003-z.
103. Id, R. S. *et al.* Seasonal patterns of dengue fever in rural Ecuador : 2009-2016. 2009–2016 (2019).
104. Guo, R. N. *et al.* The prevalence and endemic nature of dengue infections in Guangdong, South China: An epidemiological, serological, and etiological study from 2005-2011. *PLoS One* **9**, (2014).
105. Morales, I., Salje, H., Saha, S. & Gurley, E. S. Seasonal Distribution and Climatic Correlates of Dengue Disease in Dhaka , Bangladesh. **94**, 1359–1361 (2016).
106. Polwiang, S. The time series seasonal patterns of dengue fever and associated weather variables in Bangkok (2003-2017). 1–10 (2020).
107. Halstead, S. B. Dengue virus-mosquito interactions. *Annu Rev Entomol* **53**, 273–291 (2008).
108. Stewart-ibarra, A. M. & Lowe, R. Climate and Non-Climate Drivers of Dengue Epidemics in Southern Coastal Ecuador. **88**, 971–981 (2013).
109. Zhang, Q. *et al.* Epidemiology of dengue and the effect of seasonal climate variation on its dynamics : a spatio-temporal descriptive analysis in the Chao-Shan area on China ' s southeastern coast. (2019) doi:10.1136/bmjopen-2018-024197.
110. Recker, M. *et al.* Immunological serotype interactions and their effect on the epidemiological pattern of dengue. *Proceedings of the Royal Society B: Biological Sciences* **276**, 2541–2548 (2009).
111. Wagner, C. E. *et al.* Climatological , virological and sociological drivers of current and projected dengue fever outbreak dynamics in Sri Lanka. (2020).